


The influence of lithology and climatic conditions on the groundwater quality in the semi-arid-regions: case study of the Eastern Middle Cheliff alluvial aquifer (north-western Algeria)

L'influenza della litologia e delle condizioni climatiche sulla qualità delle acque sotterranee nelle regioni semi-aride: caso studio dell'acquifero alluvionale del Medio Cheliff Orientale (Algeria nord occidentale)

Elaid MADENE^a, Abdelmadjid BOUFEKANE^b , Bilal DERARDJA^c, Gianluigi BUSICO^d, Mohamed MEDDI^a

^a GEE Research Laboratory, Ecole Nationale Supérieure d'Hydraulique de Blida, Blida, Algeria

^b Geo-Environment Laboratory, Department of Geology, Faculty of Earth Sciences and Country Planning, University of Sciences and Technology Houari Boumediene (USTHB), Bab Ezzouar, 16111, Algiers, Algeria - email  : boufekane_ab@yahoo.fr

^c Centre International de Hautes Etudes Agronomiques Méditerranéennes (CIHEAM)- Mediterranean Agronomic Institute of Bari, 70010 Valenzano, Bari, Italy

^d DiSTABiF-Department of Environmental, Biological and Pharmaceutical Sciences and Technologies, Campania 7 University "Luigi Vanvitelli", Via Vivaldi 43, 81100 Caserta, Italy

ARTICLE INFO

Ricevuto/Received: 15 April 2023

Accettato/Accepted: 26 October 2023

Publicato online/Published online:

04 December 2023

Handling Editor:

Mara Meggiorin

Citation:

Madene, E., Boufekane, A., Derardja B., Busico, G., Meddi, M. (2023). The influence of lithology and climatic conditions on the groundwater quality in the semi-arid-regions: case study of the Eastern Middle Cheliff alluvial aquifer (north-western Algeria) *Acque Sotteranee - Italian Journal of Groundwater*, 12(4), 19 - 36
<https://doi.org/10.7343/as-2023-671>

Correspondence to:

Abdelmadjid Boufekane 
boufekane_ab@yahoo.fr

Keywords: groundwater quality, hydrochemistry, evaporation, rainfall, nitrate, Eastern Middle Cheliff aquifer.

Parole chiave: qualità delle acque sotterranee, idrochimica, evaporazione, precipitazioni, nitrati, acquifero del Medio Cheliff Orientale.

Copyright: © 2023 by the authors. License Associazione Acque Sotteranee. This is an open access article under the CC BY-NC-ND license: <http://creativecommons.org/licenses/by-nc-nd/4.0/>

Riassunto

Negli ultimi anni, la pianura orientale del Medio Cheliff ha assistito ad una notevole crescita economica, in particolare nel settore agricolo. Tuttavia, lo sfruttamento eccessivo della falda acquifera alluvionale, abbinato alle pratiche agricole caratterizzate dall'uso di fertilizzanti e pesticidi, ha contribuito in modo significativo al degrado della qualità delle acque sotterranee. L'obiettivo principale di questo studio è comprendere i meccanismi che governano la chimica della falda acquifera alluvionale del Medio Cheliff Orientale. Un totale di 42 campioni è stato raccolto e analizzato durante i due periodi siccitosi del 2012 e del 2017. L'elaborazione e la rappresentazione dei dati ha incluso l'analisi delle componenti principali (PCA), il diagramma di Piper, la classificazione di Stabler, i diagrammi binari, gli indici di scambio ionico, gli indici di saturazione e alcuni metodi geostatistici. L'interpretazione di questi dati ha evidenziato i seguenti risultati: i) le acque sotterranee in entrambi i periodi siccitosi del 2012 e del 2017 sono caratterizzate dalla presenza di due facies idrochimiche dominanti, cloruro di calcio e cloruro di sodio, come indicato dai diagrammi di Piper e Stabler ii) la qualità idrochimica delle acque sotterranee varia all'interno della falda acquifera, da discreta a scarsa nelle regioni orientali e centrali, con la presenza di alcuni contaminanti derivanti dall'applicazione in attività agricole di nitrati. La qualità delle acque sotterranee è classificata come molto scarsa nella regione occidentale, principalmente a causa dell'elevata salinità dovuta alla litologia dell'acquifero, alla risalita di acqua salata profonda attraverso la faglia di Cheliff dovuta al terremoto del 1980 e a due fattori climatici, l'evaporazione e le precipitazioni. Nel complesso, questo studio fornisce nuove informazioni sulle dinamiche chimiche dell'acqua della falda acquifera alluvionale del Medio Cheliff Orientale, evidenziando le diverse facies idrochimiche e l'impatto delle attività agricole e dei fattori climatici sulla qualità delle acque sotterranee nelle diverse aree della falda acquifera.

Abstract

Over the last few years, the Eastern Middle Cheliff plain has witnessed remarkable economic growth, particularly in the agricultural sector. However, the overexploitation of the alluvial aquifer, coupled with agricultural practices involving the use of fertilizers and pesticides, significantly contributed to the degradation of groundwater quality. The primary objective of this study is to comprehend the mechanisms governing the water chemistry of the Eastern Middle Cheliff alluvial aquifer. A total of 42 samples were collected and analyzed during the dry periods of the 2012 and 2017. The data processing and representation involved the utilization of analytical tools including Principal Component Analysis (PCA), Piper diagram, Stabler classification, binary diagrams, base exchange indices, saturation indices, and geostatistical methods. The interpretation of these data revealed the following findings: i) the groundwater in both the dry periods of 2012 and 2017 is characterized by the presence of two dominant hydro-chemical facies, namely calcium chloride and sodium chloride, as indicated by the Piper and Stabler diagrams; ii) the hydrochemical quality of the groundwater varies across different regions of the aquifer, fair to poor in the eastern and central regions, with the presence of certain contaminants resulting from the application of nitrates in agricultural activities. The quality is classified as very poor in the western region, primarily due to high salinity influenced by the lithology of the aquifer, the rise of deep salty water through the Cheliff fault due to the earthquake of the year 1980 and possibility by two climatic factors, namely evaporation and rainfall. Overall, this study provides new insights into the water chemistry dynamics of the Eastern Middle Cheliff alluvial aquifer, highlighting the varying hydrochemical facies and the impact of agricultural activities and climatic factors on groundwater quality in different areas of the aquifer.

Introduction

Groundwater is extensively utilized for domestic, irrigation and industrial purpose all over the world and uses especially in arid and semi-arid regions (Erostate et al., 2019; Busico et al., 2020; Taherian & Joodavi, 2021; Khan et al., 2023).

Consequently, a sustainable management of these resources to achieve a suitable groundwater quality for all kind of utilization have garnered significant attention (Prabakaran et al., 2020, Lentini et al., 2022). However, the overexploitation of groundwater is a common issue driven by population growth, resulting in increased demand for drinking water and irrigation which leads to a decline in groundwater levels and deterioration in groundwater quality (Khan et al., 2022).

In the Mediterranean basin, the exploitation rates of surface water and groundwater are exceptionally high, particularly in Maghreb countries such as Algeria (67%) and Tunisia (70%) (FAO, 2016; El Jihad & Taabni, 2019). Groundwater in Algeria is crucial for irrigation purposes but is threatened by pollution reaching alarming levels, emphasizing the critical importance of studying water quality (FAO, 2016; Busico et al., 2019).

Several hydro-geochemical studies concerning groundwater made in the Mediterranean basin, reveals degraded water quality in several countries (Boufekane et al., 2022). Alluvial aquifers are usually contaminated by natural factors (geological effects) as well anthropogenic factors (overexploitation, uncontrolled urban effluents, and intensive use of chemical fertilizers in agriculture) as stated by numerous investigation conducted in Algeria (Rezig et al., 2021; Bekhouche et al., 2022), Morocco (Mehdaoui et al., 2019; Alilouch et al., 2020), Tunisia (Jawadi et al., 2020), Italy (Vespasiano et al., 2021; Orecchia et al., 2022) and Greece (Kanellopoulos & Argyraki, 2022).

The Eastern Middle Cheliff basin has experienced significant population growth in recent decades, leading to increased water demand for urban, agriculture, and industry sectors. Water resources in this region primarily rely on the Mio-Plio-Quaternary alluvial aquifer and surface water from dams. It is noteworthy that the Eastern Middle Cheliff alluvial aquifer satisfies over 50% of the region's water use requirements. However, these water resources are subject not only to overexploitation but also to quality degradation caused by leaching of evaporitic formations following a major earthquake on October 10, 1980, which resulted a large fault. This tectonic event released deep water, which ascended to the alluvial aquifer in the El Attaf sector, of wadi Tikazale sub-basin (IFES, 2002). These factors alter the water chemistry and render it unsuitable for the desired uses, such as domestic and agricultural purposes.

Furthermore, water quality information is a crucial parameter, especially for decision-making regarding well locations and their purpose (Khan et al., 2020). Moreover, in the specific region under consideration, studying water quality becomes even more critical to the semi-arid climate (Ait Lemkademe et al., 2023), low precipitation levels, and continuously increasing water needs. Therefore, understanding the chemistry and quality of groundwater is essential for

determining its suitability for drinking, irrigation and industrial purposes (Mastrocicco et al., 2022; Johnbosco et al., 2023).

This study builds upon previous works conducted in the study area by Maghraoui (1982), Bouzelboudjen (1987), Richa (2010), and Messelmi (2012). The main objective of this study are twofold: i) to enhance the findings presented in these previous works and acquire new knowledge, and ii) to comprehend the mineralization process and hydrodynamics of the aquifer. To achieve these objectives, chemical tools were employed during two distinct periods, the dry periods of 2012 and 2017. The aim was to gain a better understanding of the influence of climatic and lithological parameters on the groundwater quality and optimize the interpretation of physico-chemical analysis through techniques (Al-Mashreki et al., 2023) such as Principal Component Analysis (PCA), Piper diagram, Stabler classification, binary diagrams, base exchange indices, saturation indices, and geostatistical methods.

Material and methods

General overview of the study area

The Eastern Middle Cheliff Basin is located southwest of Algiers and is part of the Cheliff watershed to the northeast of the latter (Fig. 1). However, Eastern Middle Cheliff plain is located from 35°30'10" to 36°25'12" N latitude and 01°35'12" to 02°37'08" E longitude. It is limited to the North by the marl and allochthonous marls of the Upper Cretaceous of Jebel BouMaad and the reliefs of Dahra. To the South, the plain is limited by the first foothills of the Ouarsenis marl-clay-sandstone massif. To the East and West, it is respectively limited by the Upper Cheliff and the Middle Cheliff Occidental basins.

The Eastern Middle Cheliff plain covers an area of approximately 360 km² and has an annual groundwater reserve estimated at 16 million m³, as reported by the National Water Resources Agency (NWRA). This groundwater resource is crucial for providing domestic, agricultural and industrial water to the cities in the region (NWRA, 2015).

The study area is surrounded by mountains, with elevation ranging from 1969 m to 531 m above mean sea level. On the opposite, the plain is relatively flat, with elevation ranging from 436 m to 63 m above mean sea level from east to west. This topography creates a gentle slope that facilitates runoff towards depressions and wadis dry river beds. The average slope in the area is approximately 0.25%. This morphology plays a significant role in the formation of a significant alluvial aquifer in the region. It is characterized by a hot-summer Mediterranean climate (Csa) (Köppen climate classification) with an annual average temperature ranging from 13.75 to 18.50 °C and a monthly maximum temperature recorded in August with more than 29 °C (Madene et al., 2020). The average annual rainfall varies between 420 and 520 mm. It is more concentrated in the altitudes on the southern mountainside of Dahra and Zaccar, and northern mountainside of Ouarsenis with an average annual rainfall of

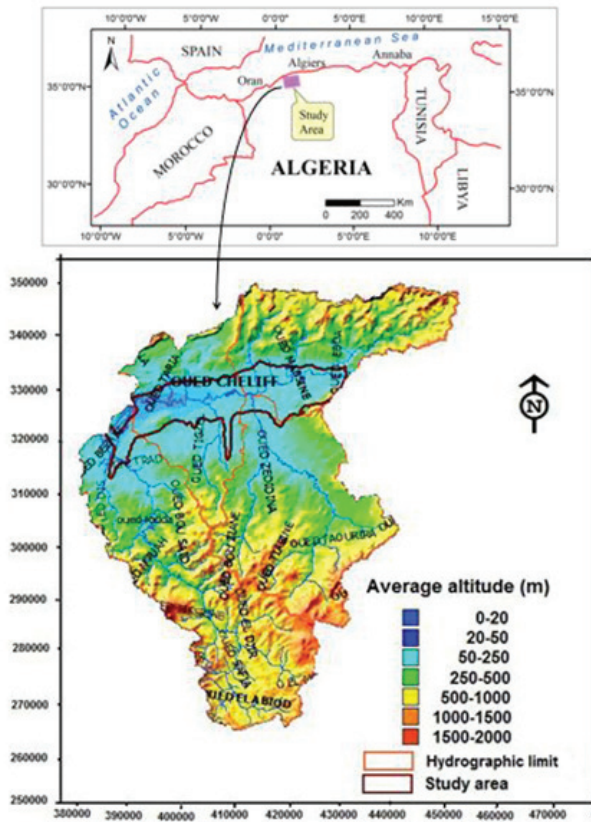


Fig. 1 - Location map of the Eastern Middle Cheliff study area.
 Fig. 1 - Carta dell'area di studio della pianura orientale del Medio Cheliff.

over 600 mm. Rainfall is lower in the Eastern Middle Cheliff plain where it varies between 300 and 400 mm (Madene et al., 2022). In winter, the region experiences spectacular flooding of the Cheliff wadi and its tributaries (Madene et al., 2020). The construction of the dams of Ouled Mellok, Oued Fodda, Harreza and Sidi Mhamed Ben Taiba allowed to regulate the flow of the wadis and to provide water for irrigation, for the period from April to November. Based on data recorded at Ain Defla weather station over a period of 45 years (1972-2017), the average annual rainfall was estimated at 439 mm. Only 23 mm (5%) infiltrate to the aquifer, while the rest is in the form of evapotranspiration with 379 mm (87%) and runoff with 37 mm (8%).

Geology and Hydrogeology

The Eastern Middle Cheliff plain located in the area of the septentrional "Tell" that corresponds to a large synclinorium Neogene and Quaternary in which have accumulated nearly 300 m of sediments. To the north, this depression is separated from the sea by the septentrional Tell represented by a series of parallel mountains from the Jurassic-Cretaceous formations that are also found in the plain (Dahra, BouMaad, Doui, Rouina and Temoulga). To the south, the basin of the Eastern Middle Cheliff plain is limited by the meridional "Tell" represented by a set of mountainous massif where the substratum is mainly marl and limestone of the Ouarsenis massifs (Perrodon 1957; Mattaeur 1958; Boulaine 1957;

Kireche 1977; Maghraoui 1982). It is penetrated in the East by the threshold of Doui and it comes out in the West by the threshold of Oum Drou. It is constituted by Helvetian marls (Fig. 2).

From the lithostratigraphy, the Eastern Middle Cheliff depression is constituted in its entirety by the formations of Mio-Plio-Quaternary age. The lithological cross-sections made in this region show the synclinal aspect of the various geological formations (Fig. 3). It is the formations of the Miocene rests in discordance on the sandstone and clay of the lower Cretaceous. It is constituted by puddings and sandstones surmounted by limestones with Lithothamnium forms the lower Miocene. The upper Miocene is constituted at the base of bluish clayey marls with sandstone intercalations (Helvetian) (Bouzelboudjen, 1987). Sandstone has been attributed to the lower Pliocene or marine Pliocene. The sandstone is often pulverulent with calcareous cement and

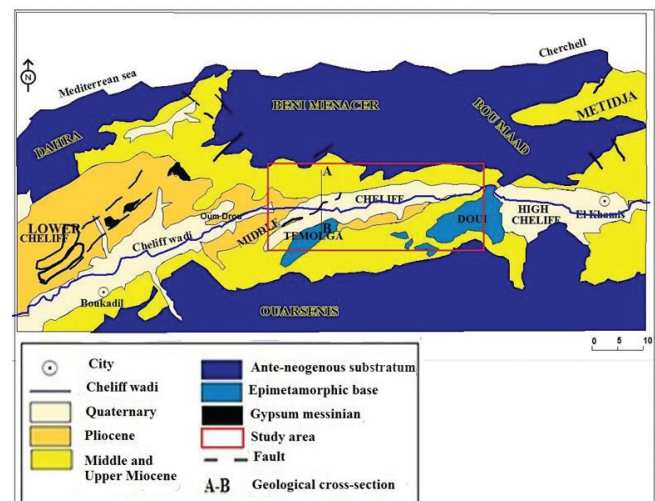


Fig. 2 - Simplified geological map (Perrodon 1957 and Mattaeur, 1958).
 Fig. 2 - Carta geologica semplificata (Perrodon 1957 e Mattaeur, 1958).

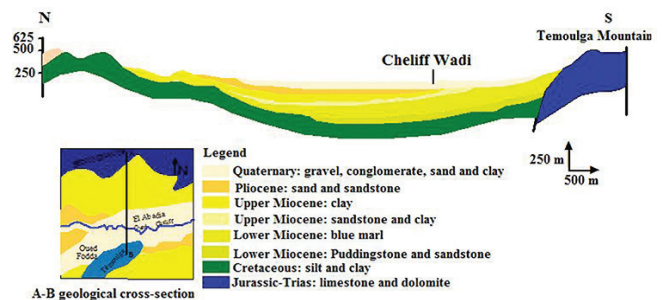


Fig. 3 - Geological section in the Eastern Middle Cheliff plain.
 Fig. 3 - Sezione geologica della pianura orientale del Medio Cheliff.

can locally change to sandstone limestones (Remaoun, 2007).

The quaternary formations cover large areas in the valley of the Eastern Middle Cheliff plain which is constituted by coarse alluvium, essentially pebble, conglomerate, gravel and sand interspersed with clay. The quaternary alluvium that constitutes an important groundwater reservoir is very heterogeneous, composed of sandy silt, clayey pebble and gravel. The thickness of the quaternary alluvium at the center study area, that corresponds to "El Abadia", is of 138 to 175 m. In addition, the thickness is considerably reduced to reach 15 to 40 m in the upstream part of the study area (Bouzelboudjen, 1987).

The observation of the piezometric map morphology for the dry periods 2012 and 2017 indicates that the piezometric level is decreasing from East to West. Thus, the general flow direction of the groundwater is East-West that coincides substantially with the course of the Cheliff wadi (Fig. 4). The piezometric curves show that the groundwater is laterally recharged and converges to feed the Cheliff wadi in center. It is important to mention that the wadi direction represents the main drainage axis. The region between Rouina and Ain Defla, and the central region between Rouina and El Attaf correspond to the tight piezometric curves indicating a strong hydraulic gradient. It is of the order of 1.1×10^{-2} to 3.2×10^{-2} . The variation in the hydraulic gradient is due, essentially, to the heterogeneity of the lithology owing to the rising of Miocene clayey substratum. Examination of the 2012 and 2017 dry periods piezometric maps shows

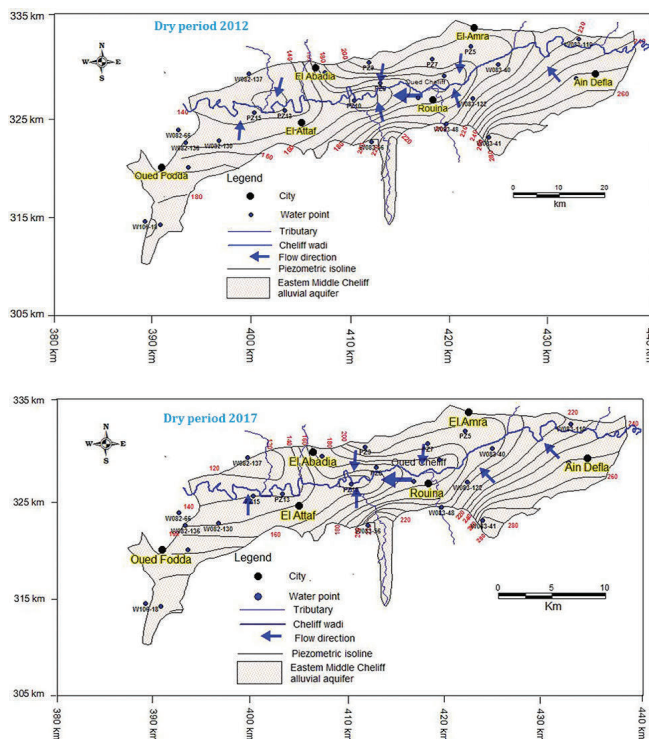


Fig. 4 - Piezometric maps during dry periods 2012 and 2017.

Fig. 4 - Mappe delle superfici piezometriche durante i periodi siccitosi del 2012 e 2017.

no change in piezometric morphology between the years, reflecting the same flow regime. However, some fluctuation in the piezometric surface can be noticed in the center of the aquifer, as well as some disturbances due to the intensive overexploitation of the aquifer for irrigation.

Method and data used

Figure 5 shows the general flowchart that summarizes the methodology utilized in this study. A sampling network was selected to acquire representative data on the spatial and temporal variability of the Eastern Middle Cheliff alluvial aquifer quality. The water samples are taken by the National Water Resources Agency from wells and piezometers covering the whole plain. The study is based mainly on sampling information from 24 water points (16 wells and 8 piezometers).

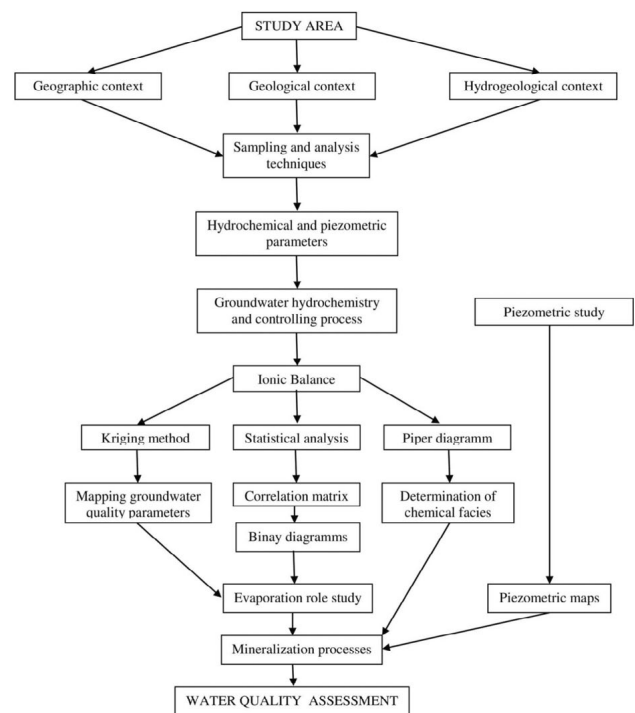


Fig. 5 - Flowchart of the methodology presented in this study.

Fig. 5 - Diagramma di flusso della metodologia presentata in questo studio.

Two campaigns were conducted in 2012 and 2017 for dry periods to analyze the physico-chemical parameters. Groundwater samples were collected after pumping water for 10 to 15 minutes. These samples were taken in 250 mL polyethylene bottles for physico-chemical analysis, kept in a cooler and analyzed immediately after the sampling campaign in the National Water Resources Agency laboratory. The analyses focused on the most common and abundant ions in groundwater. These are four cations (Ca^{2+} , Mg^{2+} , Na^+ , K^+) and four anions (Cl^- , HCO_3^- , SO_4^{2-} , NO_3^-), as well as the dry residue, temperature (T), electrical conductivity (EC) and pH.

The temperature, pH, EC were measured in situ immediately after collection using WTW ProfiLine 340i Universal Multi-parameter portable instrument (± 0.1 °C, ± 0.01 pH and $\pm 1\%$

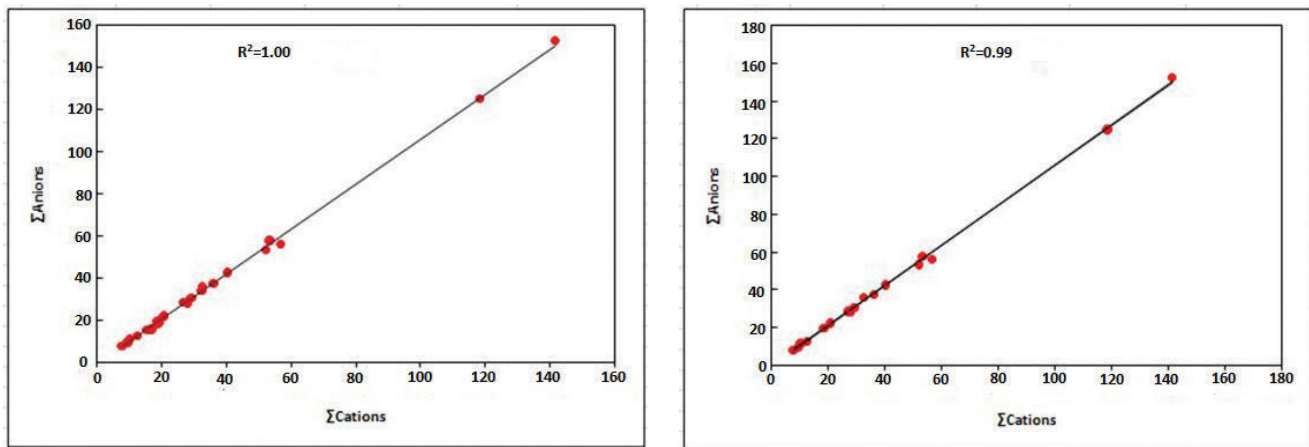


Fig. 6 - Correlation between sum of anions and cations.

Fig. 6 - Correlazione tra le somme di anioni e cationi.

CE). The filtered and acidified (1% v/v) HNO_3 were analyzed for cations (Ca^{2+} , Mg^{2+} , Na^+ , K^+) by a multi-parameter device (atomic absorption spectrophotometry). The hydrochemical analyses (cations and anions) were carried out using a UV spectrophotometer, a turbidimeter and a colorimeter in the NWRA laboratory.

The processing and representation of data involved the use of classical and modern tools such as: Piper diagrams, Stabler classification, binary diagrams, base exchange indices, saturation indices, statistical analysis (PCA), and geostatistics (mapping). For the reliability of the results analysis, the ionic balance method was applied and an error of 5% was accepted. Indeed, the correlation of absolute contents in major elements gives a good correlation coefficient: $R^2 = 1$ and $R^2 = 0.99$ in the dry periods 2012 and 2017, respectively (Fig. 6).

Results and discussion

Statistical analysis of chemical data

In most cases, the standard deviation of the different elements is lower than the mean, this indicates that the values of the variables are not very dispersed (Tab. 1). Thus,

it reflects certain hydro-chemical homogeneity of the water sampled in the study area. The coefficient of variation is high for Ca^{2+} , Mg^{2+} and SO_4^{2-} , and even very high for Na^+ , K^+ , Cl^- and NO_3^- , indicating a significant spatial variability (spatial heterogeneity). Therefore, a need for a spatial study.

From the analysis of the correlation matrix (Tab. 2), most of the variables (Ca^{2+} , Mg^{2+} , Na^+ , K^+ , and Cl^-) are intercorrelated for the two dry periods 2012 and 2017. This correlation indicates the elements evolving together that probably are of the same origin such as the couples (Na^+ - Mg^{2+}), (Ca^{2+} - Mg^{2+}), (Mg^{2+} - SO_4^{2-}) and (Na^+ - Cl^-), (Na^+ - Ca^{2+}). We notice that the dry residue is perfectly correlated to Ca^{2+} , Mg^{2+} , Na^+ , K^+ , and Cl^- . These correlations clearly identify the main elements that contribute to groundwater salinity.

NO_3^- and HCO_3^- show no correlation with some and correlated negatively with others in both periods. Less significant correlations between dry residue, HCO_3^- and NO_3^- indicate that the groundwater salinity is likely to be due to salt formations of the region (gypsum). Non-significant correlation between SO_4^{2-} and Ca^{2+} indicates that these elements may have a different origin. This latter would

Tab. 1 - The variation of the groundwater physico-chemical parameters.

Tab. 1 - La variazione dei parametri fisico-chimici delle acque sotterranee.

Element	Dry period 2012					Dry period 2017				
	Max	Min	Mean	SD	CV	Max	Min	Mean	SD	CV
Ca^{2+} (mg/L)	622	35	236	150.3	0.63	701	4	153	159.9	1.04
Mg^{2+} (mg/L)	427	18	129	90.1	0.69	109	4	55	31.83	0.58
Na^+ (mg/L)	1160	49	282	299.9	1.06	2900	110	575	743.17	1.29
K^+ (mg/L)	50	2	7	9.7	1.39	38	02	10	9.16	0.91
Cl^- (mg/L)	3890	180	796	817.7	1.02	5700	218	1017	1374.2	1.35
SO_4^{2-} (mg/L)	1180	9	344	297.2	0.86	531	4	164	154.8	0.94
HCO_3^- (mg/L)	488	31	287	136.6	0.47	474	27	262	139.4	0.53
NO_3^- (mg/l)	195	0	45.4	47.1	1.03	225.5	0	56.5	75.0	1.32
Dry residue (mg/L)	9222	622	2469	1947.7	0.78	9423	724	2294	2286.3	0.97
pH	8.3	6.8	7.6	0.37	0.04	9.4	5.1	7.7	0.94	0.12

Tab. 2 - Correlation matrix between variables.

Tab. 2 - Matrice di correlazione tra le variabili.

Variables	Ca ²⁺	Mg ²⁺	Na ⁺	K ⁺	Cl ⁻	SO ₄ ²⁻	HCO ₃ ⁻	NO ₃ ⁻	D.Res	
Ca ²⁺	1									Dry period 2012
Mg ²⁺	0.750	1								
Na ⁺	0.430	0.650	1							
K ⁺	0.440	0.670	0.688	1						
Cl ⁻	0.690	0.790	0.884	0.853	1					
SO ₄ ²⁻	0.460	0.680	0.487	0.169	0.342	1				
HCO ₃ ⁻	0.220	0.110	-0.360	-0.440	-0.320	0.263	1			
NO ₃ ⁻	0.160	0.060	-0.270	-0.260	-0.160	-0.090	0.428	1		
D.Res	0.730	0.860	0.900	0.975	0.975	0.519	-0.190	-0.110	1	
Variables	Ca ²⁺	Mg ²⁺	Na ⁺	K ⁺	Cl ⁻	SO ₄ ²⁻	HCO ₃ ⁻	NO ₃ ⁻	D.Res	
Ca ²⁺	1									Dry period 2017
Mg ²⁺	0.509	1								
Na ⁺	0.669	0.136	1							
K ⁺	-0.374	-0.351	0.366	1						
Cl ⁻	0.758	0.190	0.987	0.221	1					
SO ₄ ²⁻	0.167	0.735	-0.280	-0.349	-0.258	1				
HCO ₃ ⁻	-0.204	-0.102	-0.485	-0.065	-0.518	0.284	1			
NO ₃ ⁻	0.218	0.295	-0.248	-0.425	-0.205	0.168	0.353	1		
D.Res	0.773	0.298	0.989	0.293	0.983	-0.168	-0.463	-0.171	1	

be linked to the nature of the reservoir and to the human activities mainly linked to agriculture including the excessive use of fertilizers based on potassium sulfate, ammonium sulfate and ammonium sulfo-phosphate.

Spatial distribution of the main elements and the dry residue

The distribution of concentrations in the Eastern Middle Cheliff is influenced by several factors, including lithology, groundwater hydrodynamics, and climatic conditions. For example, high temperatures can lead to increased evaporation, while precipitation can promote leaching and dissolution of rocks (Ghebouli et al., 2008).

Regarding the spatial distribution of the dry residue during the two periods under study, relatively low values are observed upstream of the aquifer compared to the downstream areas (refer to Fig. 7 and Fig. 8). The region between El Amra and El Abadia exhibits the lowest values, with concentrations of less than 1000 mg/L. On the other hand, the El Attaf region (Jebel Temoulga) shows higher dry residue values ranging between 3000 and 10000 mg/L, representing the highest values concentrations. Additionally, the spatial distribution pattern of Cl⁻, Ca²⁺, Mg²⁺, Na⁺ and dry residue is relatively similar (see Fig. 7 and Fig. 8). The highest concentrations of these elements are observed at the El Attaf region, which may be attributed to the influx of water from the surrounding areas.

The chloride ion serves as an effective indicator of surface pollution in non-coastal areas. Observation of the chloride maps (Fig. 7 and Fig. 8) reveals its abundance in the groundwater of the Eastern Middle Cheliff plain, with

over 90% of the water points showing a chloride chemical trend. These levels exceed the Algerian standards set at 250 mg/L. Significant concentrations of chlorides have been recorded upstream of the aquifer, between the cities of Ain Defla and Rouina. The proximity to marly Miocene land and the effect of surface leaching during heavy rains, combined with evaporation due to the shallow depth of the piezometric surface (not exceeding 5 m), are likely contribution factors to these elevated chloride concentrations.

Moreover, high chloride content in groundwater is also present in the El Attaf region, near to the Jebel Temoulga. This can be attributed to the upward movement of deep saline water along the NW-SE fault that truncates the extremity of Jebel Temoulga, where Triassic or Permo-triassic formations are present (IFES, 2002). The concentration of sulfates in natural water exhibits considerable variability, influenced by the solubility of gypsum formations. In the studied area, this variability is attributed to the use of sulfate chemical fertilizers, wastewater, and industrial effluents containing sulfuric acid (H₂SO₄) as well as leaching of clayey and marly soils. The highest concentrations are recorded during the dry period 2012, in the south of Oued Fodda city (Fig. 7). They are, probably, due to the leaching of the evaporitic deposits in the region.

The maximum values of bicarbonates are encountered in the southeast of Ain Defla (foothills of the Doui massif) and in the southwest of Oued Fodda, as well as in the Rouina region, in the south (foothills of the Rouina massif). The high values can be explained by the dissolution of carbonate

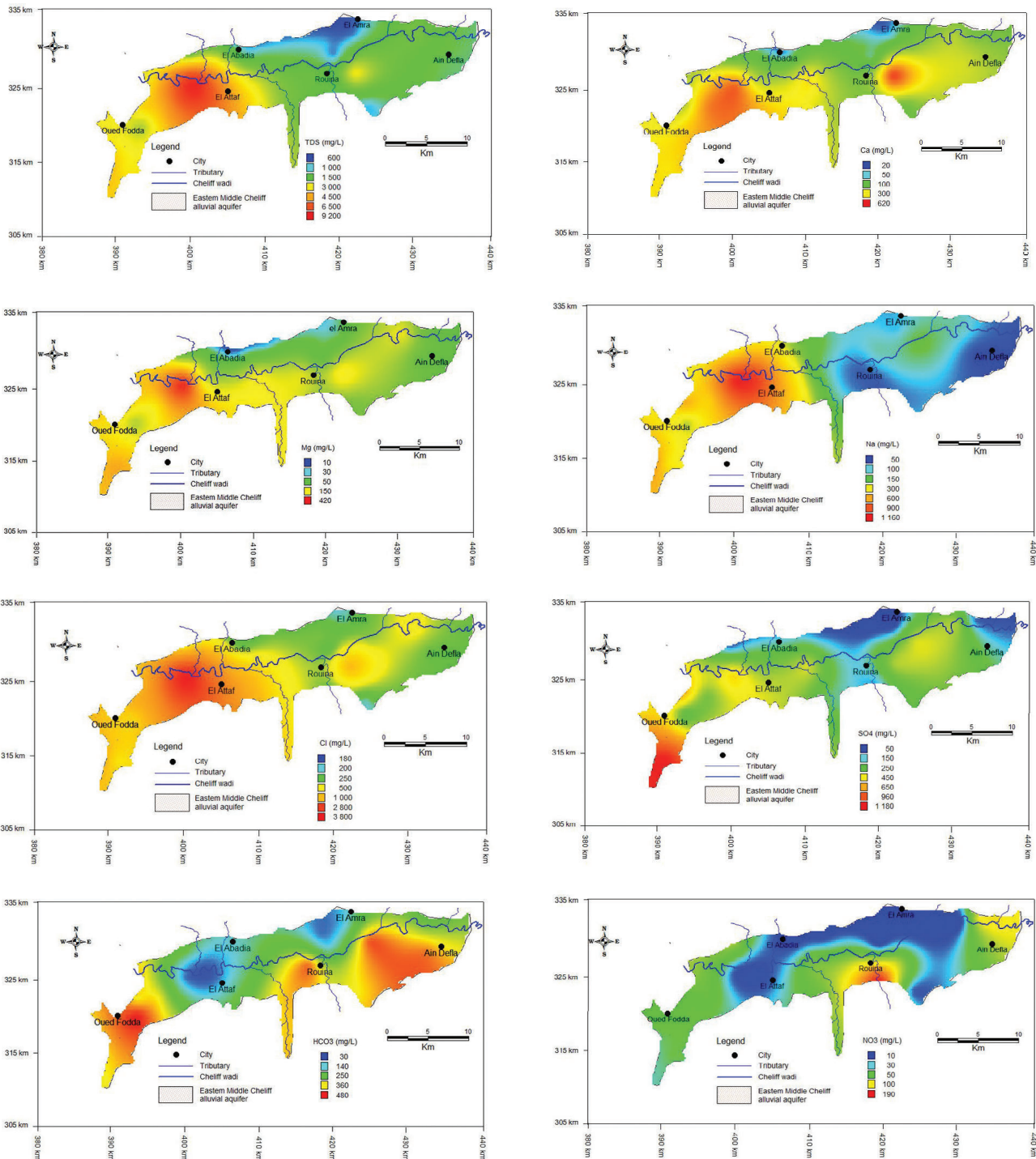


Fig. 7 - Spatial distribution of TDS, Ca²⁺, Mg²⁺, Na⁺, Cl⁻, SO₄²⁻, HCO₃⁻, and NO₃⁻ for the dry period 2012.

Fig. 7 - Distribuzione spaziale delle concentrazioni di TDS, Ca²⁺, Mg²⁺, Na⁺, Cl⁻, SO₄²⁻, HCO₃⁻, e NO₃⁻ per il periodo siccitoso del 2012.

minerals. Furthermore, it is noted that in some points, the concentrations are relatively high during the dry period of 2012, due to the dissolution of limestones providing bicarbonates accelerated by the irrigation practices using water of from Ouled Mellok and Oued Fodda dams.

Given that the Eastern Middle Cheliff alluvial aquifer is primarily used for agricultural purposes, it is expected that the presence of nitrates in the water is mainly due to

the application of fertilizers and discharge of wastewater effluent. Nitrate level mapping during the two periods (2012 and 2017) (refer to Fig. 7 and Fig. 8) reveals that the highest concentrations are found in the south region (near Rouina city) and in the northeast of the plain (near Mekhatria city), with concentrations exceeding 100 mg/L. On the other hand, between El Amra and El Abadia on the right bank, nitrate concentrations remain below 10 mg/L.

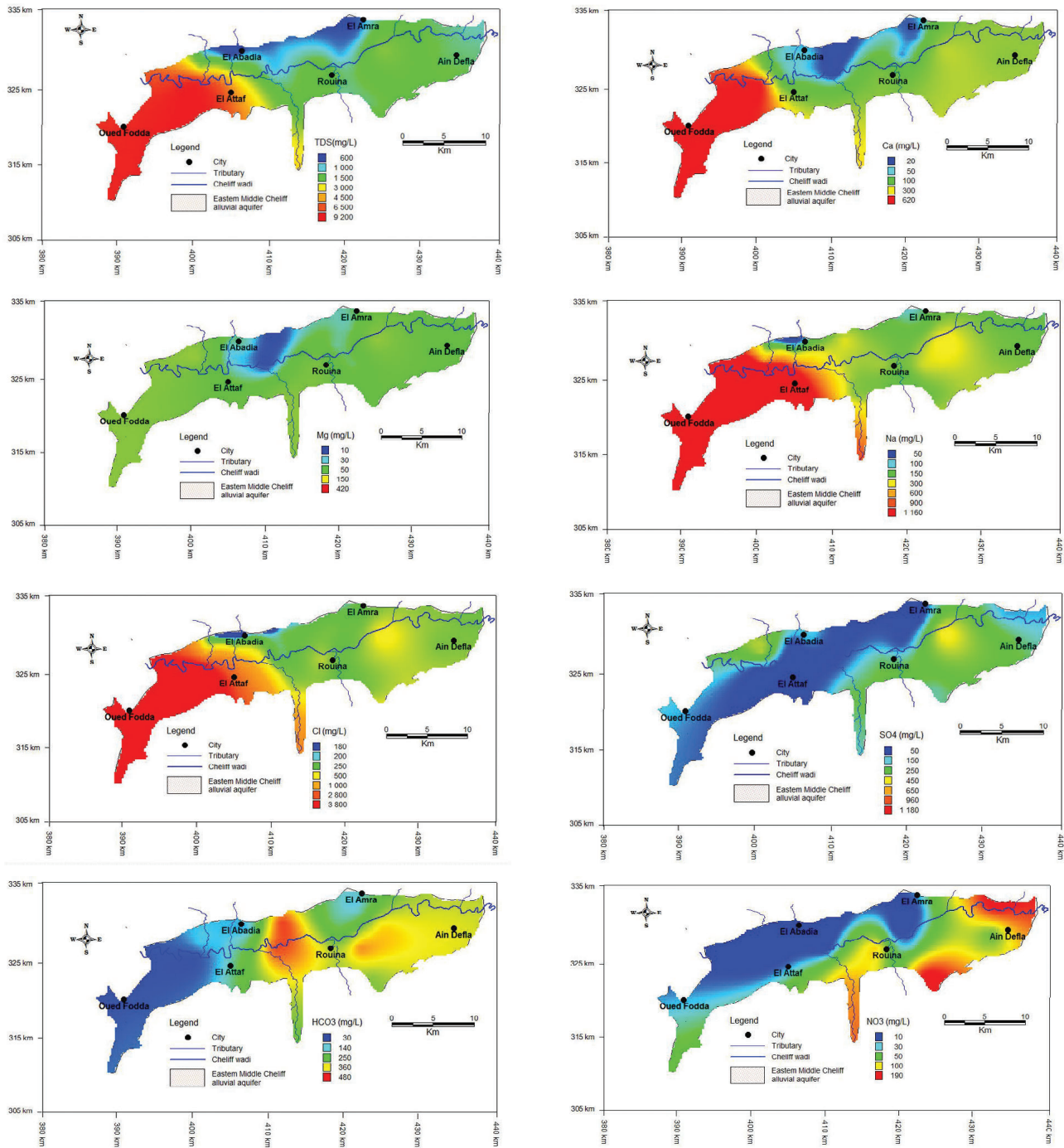


Fig. 8 - Spatial distribution of TDS, Ca²⁺, Mg²⁺, Na⁺, Cl⁻, SO₄²⁻, HCO₃⁻, and NO₃⁻ for the dry period 2017.

Fig. 8 - Distribuzione spaziale delle concentrazioni di TDS, Ca²⁺, Mg²⁺, Na⁺, Cl⁻, SO₄²⁻, HCO₃⁻, e NO₃⁻ per il periodo siccitoso del 2017.

Figure 9 indicates that nitrate ions exhibit different trends during the two observation periods. However, it can be observed that the concentrations recorded during the dry period 2017 campaign are generally higher compared to the dry period 2012 campaign.

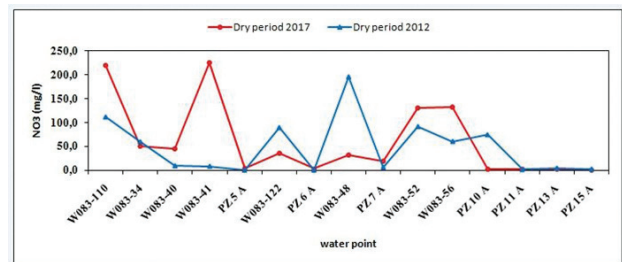


Fig. 9 - Comparison of the nitrate concentrations of the two campaigns.

Fig. 9 - Confronto delle concentrazioni di nitrati durante le due campagne di monitoraggio.

Principal Component Analysis (PCA)

The results of the analysis have introduced new hypotheses and have contributed to expanding our understanding of the problem under study (Stafford & Bodson, 2006). The various parameters analyzed in the study represent the variables that characterize the statistical units (Gouaidia, 2008). The type of analysis conducted is a reduced centered Principal Component Analysis (PCA) performed on a dataset consisting of 9 variables (Ca²⁺, Mg²⁺, Na⁺, K⁺, Cl⁻, SO₄²⁻, HCO₃⁻, NO₃⁻ and dry residue) and 48 samples collected during the two campaigns (dry periods of 2012 and 2017). The statistical processing of the data from the two surveys was performed using the software XLSTAT version 2015 and SPSS 16.0 (Al-Mashreki et al., 2023). A correlation matrix of the 9 parameters revealed strong and positive correlations, which is highly interesting. In this study, 9 factors account for 100% of the variance. However, only the factors F1, F2 and F3 were considered for interpretation, as they account for 87% and 84% of the variance, respectively. Consequently, the interpretations were focused on these three axes.

Tab. 3 - Representativeness of the factorial axes.

Tab. 3 - Rappresentatività degli assi fattoriali.

Campaign		Factorial axis 1	Factorial axis 2	Factorial axis 3
Dry period 2012	Variability (%)	56.15	20.80	10.56
	% cumulative	56.15	76,96	87.52
Dry period 2017	Variability (%)	44.66	27.78	11.31
	% cumulative	44.66	72.44	83.74

The projection of the variables on the F1-F2-F3 factorial plane shows that the F1 axis expresses 56.15% and 44.15% of the variance (Tab. 3) and it is determined by Cl⁻, SO₄²⁻, Ca²⁺, Mg²⁺, Na⁺, K⁺, and dry residue (Fig. 10). It presents the pole of the groundwater mineralization that is mostly due to the evaporite minerals that causing the salinity of water, knowing that Ca²⁺ and Mg²⁺ do not evolve with the HCO₃⁻.

Water pollution is represented on the second and the third factor (F2, F3) which contains nitrate, sulfate and bicarbonate, reflecting three distinct origins. The output of PCA presents three clusters: i) saline water characterized by dry residue exceeding 1000 mg/L and by a high concentration of Cl⁻ and Na⁺, ii) polluted water with a high concentration of NO₃⁻ and iii) alkaline water.

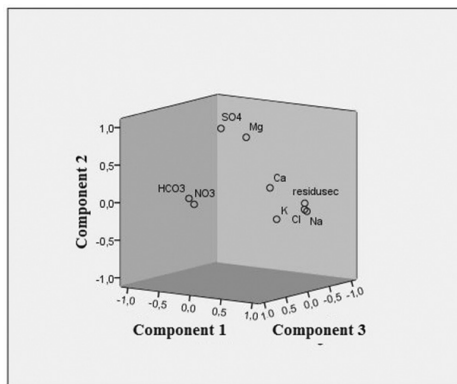
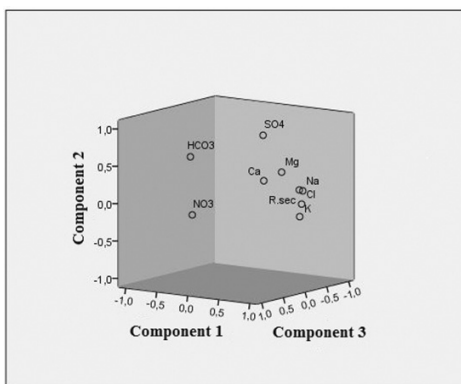


Fig. 10 - Projection of variables on the factorial plane (F1, F2 and F3).

Fig. 10 - Proiezione delle variabili sul piano fattoriale (F1, F2 e F3).

Determination of the hydrochemical facies

Hydrochemical facies are commonly employed in hydrogeology to provide a general description of the composition of natural water (Djabri, 1996; Ait Lemkademe et al., 2023). The interpretation of the hydrochemical analysis results for the two dry periods of 2012 and 2017 facilitated the monitoring of the chemical facies, their temporal variations, and the natural conditions contribution to their origin.

The use of a Piper diagram for representing the chemical elements in the samples reveals that most of the samples cluster around the poles corresponding to the chloride-calcium and chloride-magnesium facies, with some samples exhibiting characteristics of the chloride-sodium facies (refer to Fig. 11). This can likely be attributed to the dissolution of the alluvial formations from the Mio-Plio-Quaternary period, as well as evaporitic formations such as gypsiferous marls. Such dissolution processes contribute to the presence of various chemical elements, including chloride, calcium, magnesium, and sodium. However, it should be noted that this representation has the limitation of associating chloride with nitrate, which can potentially lead to misinterpretations (Touhari, 2015).

For this, the Stabler classification is useful as a complementary method to the Piper diagram, this type of classification is essential in the hydrochemical study. It

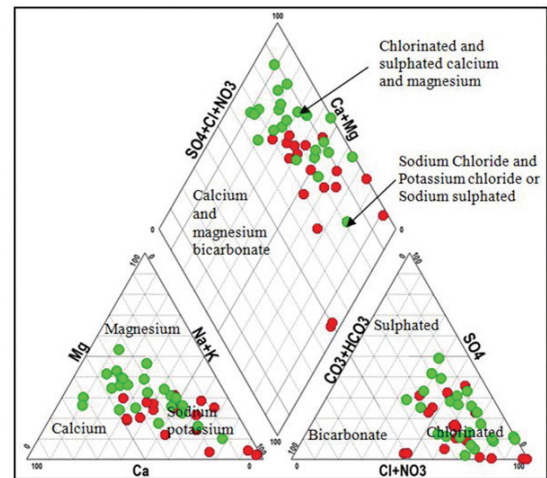


Fig. 11 - Piper diagram, (green points: dry period 2012, red points: dry period 2017).

Fig. 11 - Diagramma Piper (punti verdi: periodo siccitoso del 2012, punti rossi: periodo siccitoso del 2017).

Tab. 4 - Chemical facies of the Eastern Middle Cheliff alluvial aquifer.

Tab. 4 - Facies chimica dell'acquifero alluvionale orientale del Medio Cheliff.

Campaign	Water family	Chemical facies	(%)	(%)
Dry period 2012	Chloride	Chloride-calcium	38	W083-110
		Chloride-sodium	42	PZ 13 A
		Chloride-magnesian	8	W083-52
	Sulphated	Sulphated-magnesian	8	W082-66
		Bicarbonated	Bicarbonated-calcium	4
Dry period 2017	Chloride	Chloride-calcium	28	W083-56
		Chloride-sodium	67	PZ 12 A
	Bicarbonated	Bicarbonated-sodium	05	PZ 9 A

brings out the different water facies and allows to follow their evolution. The characteristic formula of Stabler counts on calculating the percentage of each ion in reaction, compared to the total concentration.

According to the Table 4, the chemical facies of study area is dominated by cations Ca^{2+} , Na^{2+} and anion Cl^- which explains the dominance of the chloride-sodium and chloride-calcium facies for the two dry periods 2012 and 2017.

The determination of the different facies' percentage of both dry periods 2012 and 2017 (Fig. 12) shows a certain chemical zoning related mainly to the lithological nature of the formations (lands) crossed. This has allowed highlighting two chemical facies. The first facies is the chloride-sodium, it is the most important and dominant in the western part of the study area. Also, the chloride-sodium facies develops in the El Attaf area due to the existence of Triassic saliferous formations

under the Jurassic limestones of Jebel Temoulga and the water flow through the Jurassic limestones and the deep gypso-saliferous formations (the fault offset in 1980 made these water overflow). This can explain the strong mineralization of the first group of water which then contaminate the alluvial aquifer. The second facies is the chloride-calcium characterizing the upstream and downstream zone of the Eastern Middle Cheliff aquifer. It is explained by the presence of the alluvial formations of the Mio-Plio-Quaternary and gypsiferous marls. Sulfate or bicarbonate facies are present in some areas (limited zones).

The second factor involved in the high mineralization of groundwater is the phenomenon of evaporation. It is important to mention that the semi-arid conditions of the region together with low piezometric surface depths, intensifies the effect of evaporation. The distribution of hydro-geochemical facies

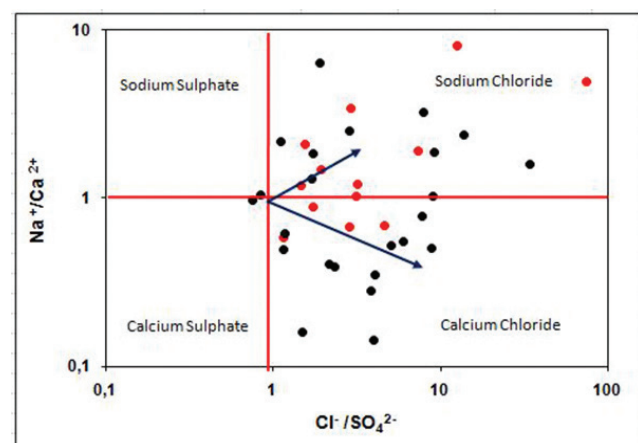
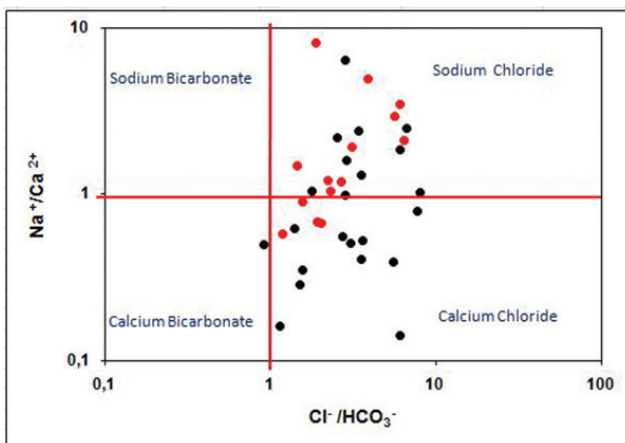


Fig. 12 - Distribution of chemical facies (black points: dry period 2012, red points: dry period 2017).

Fig. 12 - Distribuzione delle facies idrochimiche (punti neri: periodo siccitoso del 2012, punti rossi: periodo siccitoso del 2017).

appears to be conditioned by the lithology of the bedrock and anthropogenic actions.

A graphical representation of the facies, based on the quantities in reaction, is very useful for confirming their presence characterizing the groundwater of the aquifer. Given the dominance of the previous ions, two diagrams were created using the ratios $(Na^+/Ca^{2+} - Cl^-/HCO_3^-)$ and $(Na^+/Ca^{2+} - Cl^-/SO_4^{2-})$. The two diagrams illustrate the concentration of the ion ratios in 4 polls indicating the previously determined facies, that characterize the aquifer. Some chemical elements are from several different origins such as Ca^{2+} and Cl^- , and the one that influences the predominance of the facies is highlighted.

Binary diagrams and mineralization processes

To know the mechanisms of water chemistry, it is necessary to determine the origin of each element. The relationships between concentrations of the dissolved major element are shown in Figure 13. Figure 13A and 13B plot calcium as a function of sulfate and bicarbonate, respectively. The significant excess of Ca^{2+} indicates that the origin of Ca^{2+} is not only the dissolution of calcite and gypsum, and thus

confirms the hypothesis of a contribution of Ca^{2+} by ion exchange process.

The evolution of sodium is studied as a function of the chloride contents as this latter is stable tracer, conservative of evaporites and very soluble. The Na^+/Cl^- relationship has often been used to identify the mechanism of salinity acquisition.

Representing Ca^{2+} with respect to Mg^{2+} contents (Fig. 13C) mark a straight line with rectified slope, where the evolution of Mg^{2+} is independent of Ca^{2+} , indicating that the two elements evolve together. This means that Ca^{2+} and Mg^{2+} have the same origin that must be dolomites or evaporates.

In general, the presence of Cl^- and Na^+ ion in groundwater is attributed to the dissolution of halite encountered in the surrounding geological formations. However, a notable feature of the Eastern Middle Cheliff alluvial aquifer is the predominance of Cl^- over Na^+ (Fig. 13D), which are linked to another origin of this ion rather than the dissolution of halite. It can also have an anthropogenic origin (domestic and industrial effluents).

Finally, the graph representing Mg^{2+} in relation to HCO_3^- and SO_4^{2-} (Fig. 13E, 13F) showed more excess of Mg^{2+} in relation to HCO_3^- than in relation to SO_4^{2-} . This leads to

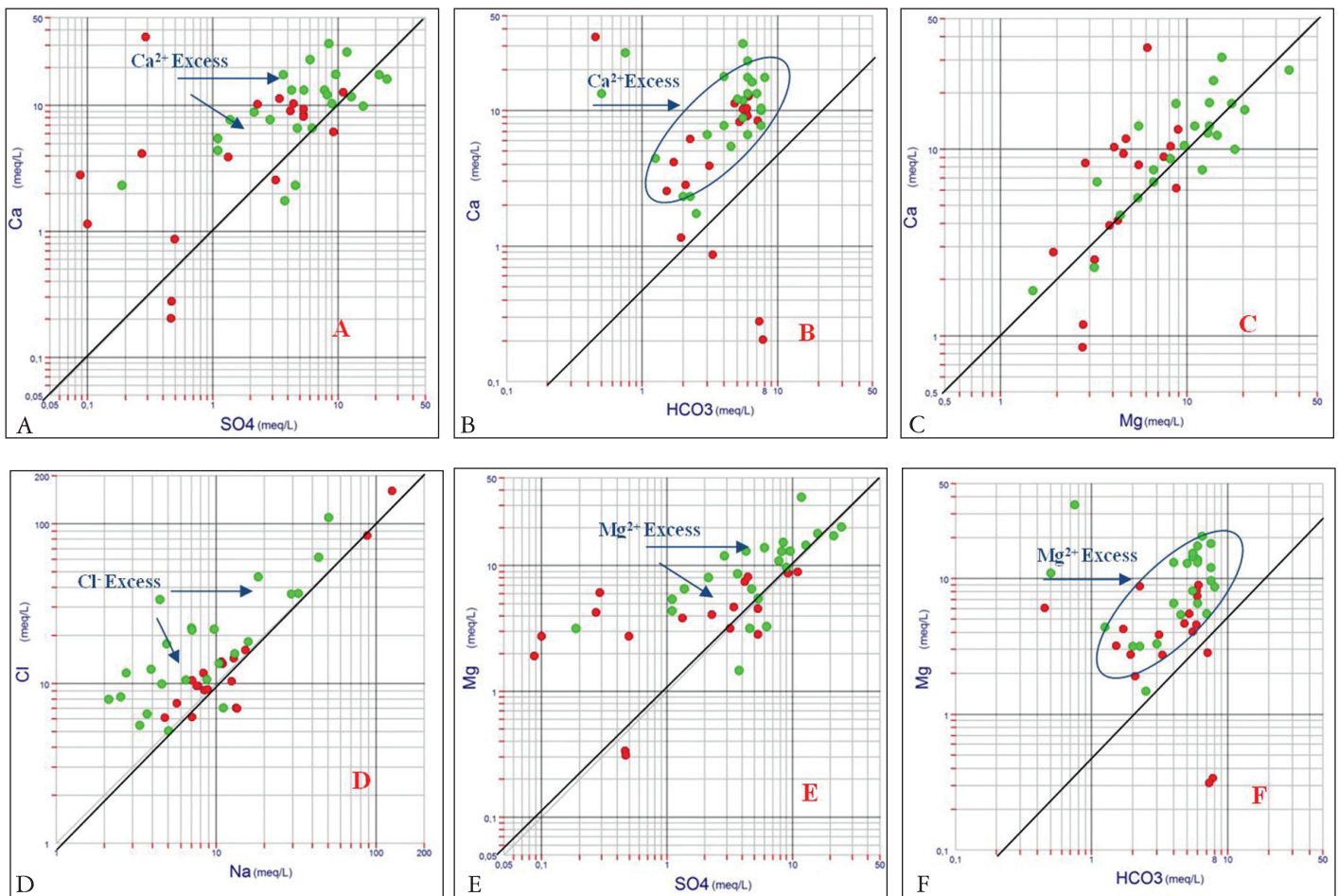


Fig. 13 - Relationships among major components (green points: dry period 2012, red points: dry period 2017).

Fig. 13 - Relazioni tra le principali componenti (punti verdi: periodo siccitoso del 2012, punti rossi: periodo siccitoso del 2017).

conclude that the Mg^{2+} originates mainly from the dissolution of dolomite.

Calculating saturation indices of the following water minerals: calcite ($CaCO_3$), aragonite ($CaCO_3$), dolomite $CaMg(CO_3)_2$, anhydrite ($CaSO_4$), gypsum ($CaSO_4 \cdot 2H_2O$) and halite ($NaCl$) in the two dry periods 2012 and 2017 show that the carbonate minerals have different degrees of saturation. Indeed, the calcite saturation index varies from -1.07 to +1.49 and -2.50 to +0.94, followed by that of aragonite from -1.21 to +1.35 and -2.64 to +0.79 and finally that of dolomite which varies from -2.09 to +3.08 and -5.59 to +2.12 in the two dry periods 2012 and 2017, respectively (Tab. 5). If the state equilibrium is admitted in the interval of -0.5 to +0.5, then the three minerals mentioned above are in a state of supersaturation for most of the water points except PZ5, PZ6, PZ7, PZ11, PZ13 and PZ15. These points present a state of undersaturation which confirms the gypsiferous origin of the calcium and not that of the carbonate. The concentrations of the three minerals have a similar evolution. The evaporitic minerals show lower saturation degrees than the carbonate minerals. Gypsum indices varies from -2.87 to -0.47 and -3.71 to -0.76, followed by anhydrite where the index varies from -3.09 to -0.69 and -3.93 to -0.98. For both gypsum and anhydrite all the wells are undersaturated. Finally, indices for the halite vary from -6.49 to -4.09 and -6.25 to -3.54 in the two dry periods 2012 and 2017, respectively. This indicates that the groundwater is undersaturated with respect to this mineral.

Similarly, Figures 14 and 15 show a positive and significant evolution between calcite and dolomite with respect to bicarbonate, gypsum and halite with respect to sulfate and chloride, respectively. This may give an indication on the dissolution of the different salts.

In summary, the thermodynamic interpretation has shown

the influence of evaporite minerals on the water chemistry. The undersaturation in gypsum, anhydrite and halite causes a continuous dissolution and an enrichment of water by these elements. In addition, the carbonate minerals are sometimes close to equilibrium and often oversaturated tending to precipitate in the form of calcite and dolomite.

Schoeller (1977) introduced the Base Exchange Index (B.E.I) as the ratio between the exchanged ions and the ions of the same nature originally existing in the water (Rodier, 1996). The interpretation of the calculated B.E.I showed that most of the plain samples have a positive index in both periods (Rodier, 2009). This dominance of the positive values translates that the surrounding rocks releases Ca^{2+} , Mg^{2+} after having fixed the Na^+ and K^+ of water. The map of the B.E.I values evolution shows that the positive values cover the entire aquifer, with the exception of some points located to the north, near to El Abadia city, presenting negative values (Fig. 16). The dominance of positive values is due to the release of Ca^{2+} and Mg^{2+} for the surrounding rocks after fixing Na^+ and K^+ from water.

The analysis of the $(Ca^{2+} + Mg^{2+})$ versus $(HCO_3^- + SO_4^{2-})$ diagram reveals that about 98% of the water points are above the line (Fig. 17), so this water has undergone the process of exchange of Na^+ from the aquifer for Ca^{2+} and Mg^{2+} from the surrounding formation ($B.E.I > 0$) and dissolution of gypsiferous formation. This is confirmed as well by the positive relationship of $(Ca^{2+} + Mg^{2+})$ versus Cl^- with a correlation coefficient $R^2 = 0.71$ (Fig. 18).

In order to characterize the effect of evaporation on the mechanism of groundwater chemistry of the Eastern Middle Cheliff alluvial aquifer, a graph that shows the relationship

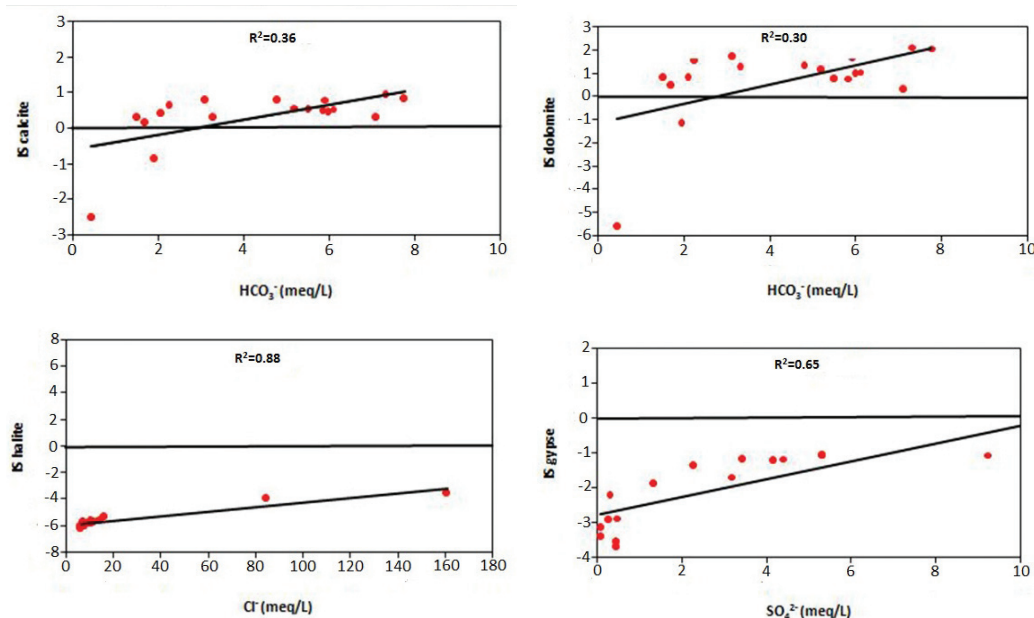


Fig. 14 - Mineral saturation indices for dry period 2012.

Fig. 14 - Indici di saturazione per il periodo siccitoso del 2012.

Tab. 5 - Evolution of mineral saturation indices.

Tab. 5 - Evoluzione degli indici di saturazione.

Dry period 2012							Dry period 2017						
Water point	Calcite	Aragonite	Dolomite	Gypsum	Anhydrite	Halite	Water point	Calcite	Aragonite	Dolomite	Gypsum	Anhydrite	Halite
PZ10	0.59	0.45	1.19	-0.73	-0.95	-5.56	PZ10	0.94	0.79	2.12	-3.56	-3.78	-5.72
PZ11	-0.34	-0.49	-0.63	-1.75	-1.97	-5.80	PZ11	0.29	0.14	0.80	-1.69	-1.91	-5.79
PZ13	-1.07	-1.21	-2.09	-0.99	-1.21	-4.36	PZ13	0.15	0.01	0.46	-2.92	-3.13	-3.93
PZ15	0.71	-0.85	-1.15	-0.75	-0.96	-4.09	PZ15	-2.50	-2.64	-5.59	-2.22	-2.44	-3.54
PZ5	0.19	-0.33	-0.11	-2.87	-3.09	-6.30	PZ5	-0.85	-1.00	-1.19	-3.42	-3.64	-6.05
PZ6	0.31	-0.46	-0.37	-1.55	-1.77	-6.28	PZ6	0.31	0.17	1.26	-2.87	-3.09	-6.04
PZ7	0.41	-0.56	-0.7	-1.92	-2.14	-6.04	PZ7	0.79	0.64	1.70	-1.9	-2.12	-5.84
PZ8	0.54	0.4	0.91	-1.09	-1.31	-5.75	PZ9	0.82	0.67	2.06	-3.71	-3.93	-5.72
W106-18	1.14	1.00	2.41	-0.52	-0.73	-4.71	PZ 12	0.42	0.27	0.81	-3.15	-3.37	-5.70
W106-19	1.43	1.28	3.08	-0.47	-0.69	-5.31	PZ 14	0.62	0.47	1.52	-1.06	-1.28	-5.47
W82-128	1.49	1.35	2.82	-1.10	-1.32	-5.42	W83-110	0.51	0.37	0.76	-1.37	-1.59	-5.85
W82-130	1.32	1.18	2.56	-0.89	-1.11	-4.85	W83-122	0.31	0.17	0.28	-1.09	-1.31	-5.62
W82-136	0.7	0.56	1.63	-0.83	-1.04	-4.74	W83-34	0.48	0.34	0.77	-1.06	-1.28	-5.84
W82-137	1.04	0.89	2.21	-1.94	-2.16	-5.42	W83-40	0.54	0.39	1.05	-0.76	-0.98	-5.36
W82-66	0.97	0.83	2.33	-0.77	-0.99	-5.61	W83-41	0.78	0.63	1.30	-1.18	-1.40	-5.85
W83-110	0.37	0.23	0.81	-1.69	-1.91	-6.03	W83-48	0.58	0.44	1.12	-1.09	-1.31	-6.25
W83-122	0.73	0.59	1.29	-0.64	-0.86	-5.61	W83-52	0.46	0.32	0.96	-1.22	-1.44	-5.57
W83-126	0.66	0.51	1.47	-0.89	-1.11	-5.81	W83-56	0.80	0.65	1.62	-1.17	-1.39	-5.57
W83-34	0.99	0.85	1.73	-0.95	-1.17	-6.49							
W83-40	0.87	0.73	1.84	-0.88	-1.10	-5.9							
W83-41	0.56	0.42	1.25	-1.22	-1.44	-6.45							
W83-48	0.65	0.51	1.40	-1.48	-1.70	-6.40							
W83-52	0.70	0.55	1.72	-1.46	-1.68	-6.22							
W83-56	0.78	0.64	1.69	-1.15	-1.37	-5.57							

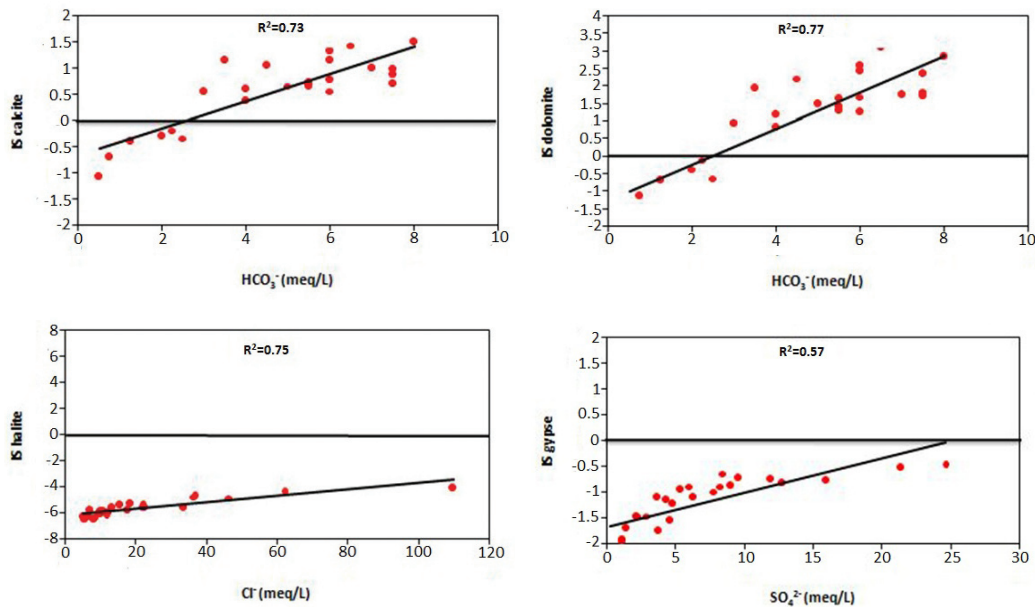


Fig. 15 - Mineral saturation indices for dry period 2017.

Fig. 15 - Indici di saturazione per il periodo siccitoso del 2017.

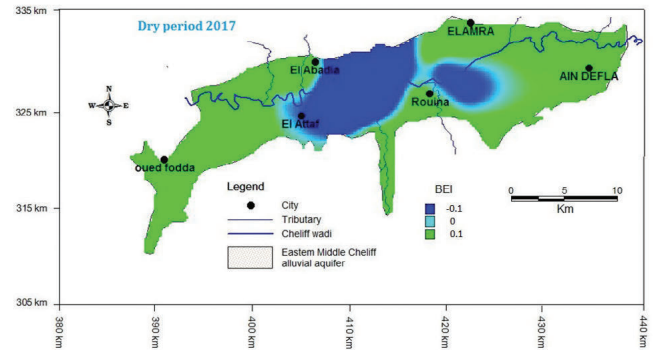
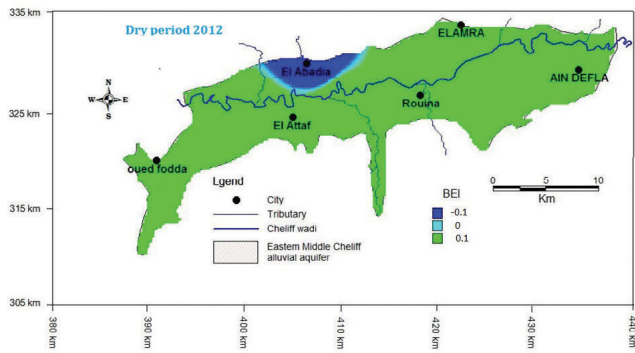


Fig. 16 - The B.E.I evolution map for dry periods 2012 and 2017.

Fig. 16 - Carta evolutiva di scambio ionico (B.E.I.) per i periodi siccitosi 2012 e 2017.

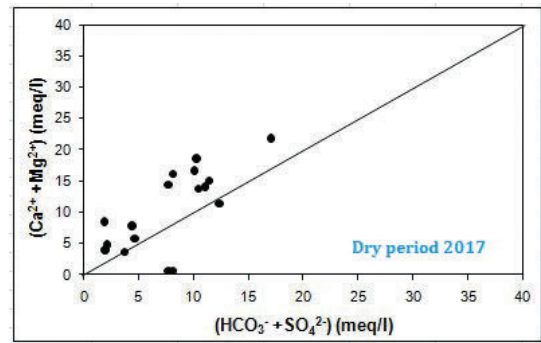
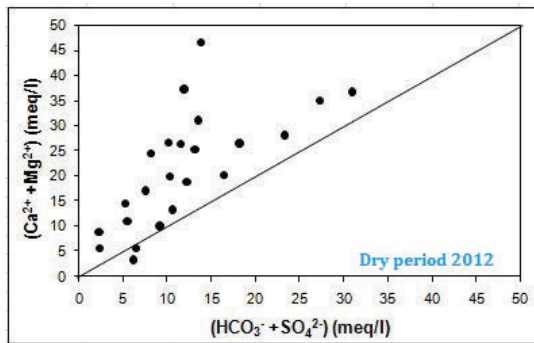


Fig. 17 - Correlation between $(Ca^{2+} + Mg^{2+})$ and $(HCO_3^- + SO_4^{2-})$ for the dry periods 2012 and 2017.

Fig. 17 - Correlazione tra le concentrazioni di $(Ca^{2+} + Mg^{2+})$ e $(HCO_3^- + SO_4^{2-})$ per i periodi siccitosi del 2012 e 2017.

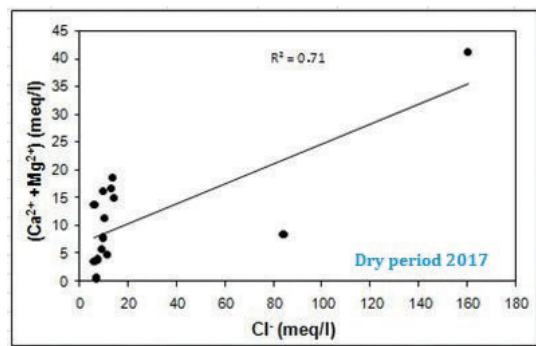
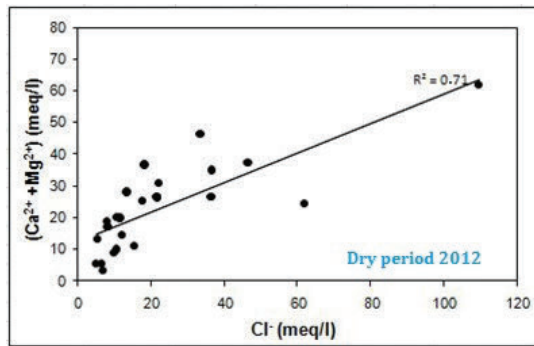


Fig. 18 - Correlation between $(Ca^{2+} + Mg^{2+})$ and Cl^- for the dry periods 2012 and 2017.

Fig. 18 - Correlazione tra le concentrazioni di $(Ca^{2+} + Mg^{2+})$ e Cl^- per i periodi siccitosi del 2012 e 2017.

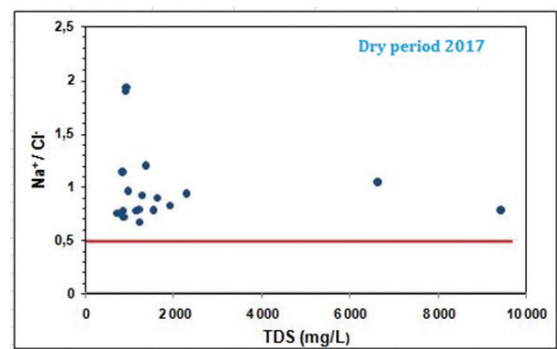
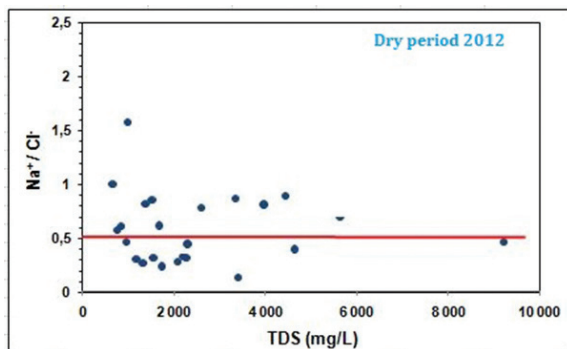


Fig. 19 - Correlation between the ratio (Na^+/Cl^-) and the dry residue.

Fig. 19 - Correlazione tra il rapporto (Na^+/Cl^-) e il residuo secco.

between the ratio (Na^+/Cl^-) and the dry residue was established (Fig. 19). Generally, it can be seen that the points are aligned on a horizontal line, i.e. that the ratio (Na^+/Cl^-) is constant in spite of the increase in dry residue contents for both dry periods 2012 and 2017, which confirm the evaporation in study area.

Groundwater use for drinking water

Groundwater often contains concentrations of various chemical elements. It is essential to ensure these concentrations do not exceed certain threshold established by the standards of the organizations such as World Health Organization (WHO) and public health services. To determine the potability of groundwater, the standards set by the World Health Organization (WHO, 2009) were considered, utilizing the Total Hydrotimetric Degree (THD). The results of the physico-chemical analysis indicate that more than 50% of the samples collected from the different water points exceed the recommended standard for water potability, except for K^+ (refer to Tab. 6).

The majority of samples in both the dry periods of 2012 and 2017 exhibit Ca^{2+} , Mg^{2+} , and Cl^- concentrations that exceed the thresholds set by the World Health Organization

(WHO). Only 13% and 22% of the samples did not exceed the WHO standard for Cl^- in the respective dry periods. However, for Nitrates (NO_3^-), more than 60% of the samples did not exceed the WHO standard in both periods. It is noting that, for the dry residue, only 38% of the samples met the WHO standard in dry period 2012, but this percentage increases to 72% in dry periods 2017. The hydrometric degree, which indicates water hardness, is determined by the sum of calcium and magnesium concentrations. Table 7 presents the analysis results for the 42 water samples. Most samples are classified as very hard for both periods, with T.H.D exceeding 54 °F. Specifically, 11% of the samples have fairly pure water, 12% and 11% have hard water, and 76 and 56% have very hard water in the dry periods 2012 and 2017, respectively. Consequently, the groundwater in the study area is considered to have poor to bad potability with only a few wells meeting the criteria for good water quality.

The spatial distribution of chemical elements in the study area confirms that the groundwater facies are strongly influenced by the lithological characteristics of the aquifer. The presence of carbonates and evaporitic formations plays a significant role in shaping the distribution of these facies. In the El Attaf area, the high mineralisation level (salinity) can be attributed to the hydraulic connection between the aquifer and the Jurassic limestones, which resulted from a tectonic fault triggered by the earthquake on October 10, 1980. This fault created an opening upstream of Jebel Temoulga, causing groundwater to overflow from the limestones through the Astian formation (Meghraoui, 1982). Furthermore, the observed increase in chloride (Cl^-) levels accompanied by low sodium (Na^+) levels can be attributed to the base exchange phenomenon. This phenomenon occurs when bedrock clays release calcium (Ca^{2+}) ions after fixing sodium (Na^+). The dominant facies in the area is the chloride-calcium facies, which extends towards the eastern and western parts of the aquifer. This distribution can be attributed to the presence of Mio-Plio-Quaternary alluvial formations and gypsiferous marls in the area.

Tab. 6 - Percentage of samples with concentrations standards (WHO, 2009).

Tab. 6 - Percentuale di campioni con concentrazioni inferiori agli standard (WHO, 2009).

Element	WHO standards	Percentage of samples with concentrations below the standards	
		Dry period 2012 (%)	Dry period 2017 (%)
Ca^{2+} (mg/L)	100	17	44
Mg^{2+} (mg/L)	50	21	44
Na^+ (mg/L)	150	50	20
K^+ (mg/L)	12	96	78
Cl^- (mg/l)	250	13	22
SO_4^{2-} (mg/L)	250	46	67
HCO_3^- (mg/L)	250	42	44
NO_3^- (mg/L)	50	63	72
TDS (mg/L)	1500	38	72
pH	6.5 < pH < 9.5	100	94

Tab. 7 - Classification of water samples according to THD.

Tab. 7 - Classificazione dei campioni d'acqua secondo THD.

T.H.D (°F)		0-7	7-14	14-22	22-32	32-54	>54
Water qualification		Very pure	pure	Moderately	Quite	Hard	Very hard
% of samples	Dry period 2012	0	0	4	8	12	76
	Dry period 2017	11	0	11	11	11	56
Domestic Use		Good potability		Fair potability		Poor potability	

Conclusion

The main findings of this work can be summarized as follows:

1. The hydrochemical analysis of 24 water samples reveals that the water in the aquifer is generally hard and highly mineralized. Based on the Piper and Stabler diagrams, two dominant chemical facies, namely chloride-calcium and chloride-sodium, are present.
2. The spatial distribution of chemical elements confirms that the origin of these facies is strongly linked to the lithological nature of the aquifer, primarily through the dissolution of carbonate and evaporitic formations. In the El Attaf region, the high mineralization is attributed to the contact between water from the alluvial aquifer and water from the Jurassic limestone.
3. Monitoring the water quality over time has demonstrated the influence of precipitation and evaporation on groundwater mineralization. A notable characteristic of the Eastern Middle Cheliff alluvial aquifer is the enrichment of chloride (Cl^-) compared to sodium (Na^+). The increase in chloride concentration, accompanied by low sodium concentration, is attributed to the phenomenon of base exchange, where bedrock clays release calcium (Ca^{2+}) ions after fixing sodium. The calculated saturation index of carbonate and gypsum minerals indicates that carbonates tend to precipitate before gypsum, allowing for the accumulation of important concentrations of chemical elements resulting from the dissolution of gypsum.
4. Through the application of Principal Component Analysis (PCA), three axes were identified. The first axis explains 56.15% and 44.15% of the total information and reflects the mineralization of water primarily influenced by geological variables (Ca^{2+} , Mg^{2+} , Na^+ , Cl^- , and K^+). The analysis reveals that groundwater to the east of the study area is weakly mineralized compared to those in the west (particularly in the El Attaf region). The high concentrations of bicarbonate and nitrate are found in the south of Rouina city (at the foothills of Jebel Rouina) and the southwest of Oued Fodda city (near Ain Defla and Mekhatria cities), respectively.
5. Furthermore, mapping of nitrate concentrations shows that the northeastern area of the Eastern Middle Cheliff alluvial plain is more exposed to pollution, with concentrations exceeding 50 mg/L. This elevated concentration can be attributed to various sources of pollution, primarily associated with agriculture, livestock, and urban practices (domestic and industrial effluents).
6. The shallow aquifer is characterized by salinity. This salinity is mainly due to the dissolution of evaporite deposits and the rise of deep salty water through the Chellif fault (due to the earthquake of the year 1980).
7. The physico-chemical analysis of the alluvial aquifer across different water points indicates that more than 50% of these points exceed the recommended standards

set by the World Health Organization (WHO) for water potability, except for potassium. The concentrations of calcium, magnesium, and chloride exceed the WHO threshold for both periods. Consequently, the high concentrations of calcium and magnesium contribute to the water being classified as very hard (with percentages of 76% and 56% in the dry periods of 2012 and 2017, respectively).

Acknowledgments

The authors would like to thank the anonymous reviewers for their comments, which helped to improve this article.

Funding source

The study is carried out within the framework of the SWATCH project (Prima project) funded by the DGRSDT, Algeria.

Competing interest

All authors, the corresponding author states that there is no conflict of interest.

Author contributions

Work and concept were initiated by Elaid Madene, Abdelmadjid Boufekane, and Mohamed Meddi. Material preparation, sample and data collection were performed by Elaid Madene and Mohamed Meddi. Data analysis was performed by Elaid Madene and Abdelmadjid Boufekane. The manuscript was written and reviewed by Elaid Madene, Abdelmadjid Boufekane, Bilal Derardja and Gianluigi Busico. All the authors read and approved the final manuscript.

Additional information

Supplementary information is available for this paper at <https://doi.org/10.7343/as-2023-671>

Reprint and permission information are available writing to acquesotterranee@anipapozzi.it

Publisher's note Associazione Acque Sotterranee remains neutral with regard to jurisdictional claims in published maps and institutional affiliations.

REFERENCES

- Alilouch, R., El Morabiti, K., El Mrihi, A., & Ouchar Al-Djazouli, M. (2020). Application of statistical methods to the hydrogeochemical study of groundwater in the Beni Hassan Dorsal (Northern Rif, Morocco). *International Journal of Innovation and Applied Studies*, 30(2), 546–562.
- Al-Mashreki, M.H., Eid, M.H., Saeed, O., Székács, A., Szűcs, P., Gad, M., Abukhadra, M.R., AlHammadi, A.A., Alrakhami, M.S., Alshabibi, M.A., Elsayed, S., Khadr, M., Farouk, M., & Ramadan, H.S. (2023). Integration of Geochemical Modeling, Multivariate Analysis, and Irrigation Indices for Assessing Groundwater Quality in the Al-Jawf Basin, Yemen. *Water*, 15, 1496. <https://doi.org/10.3390/w15081496>
- Ait Lemkadem, A., El Ghorfi, M., Zouhri, L., Heddoun, O., Khalil, A., & Maacha, L. (2023). Origin and Salinization Processes of Groundwater in the Semi-Arid Area of Zagora Graben, Southeast Morocco. *Water*, 15, 2172. <https://doi.org/10.3390/w15122172>
- Bekhouche, N., Khiel, S., Ouldjaoui, A., Ababsa, L., & Marniche, F. (2022). Qualité Physico-chimique des eaux de l'oued Sigus (Nord-Est de l'Algérie) : Caractérisation et analyse en composantes principales. "Physico-chemical water quality of Sigus wadi (North-East of Algeria): Characterization and Principal component analysis". *BioRessources*, 12, 2–11.
- Boufekane, A., Maizi, D., Madene, E., Busico, G., & Zghibi, A. (2022). Hybridization of GALDIT method to assess actual and future coastal vulnerability to seawater intrusion. *Journal of Environmental Management*, 318, 115580. <https://doi.org/10.1016/j.jenvman.2022.115580>
- Boulaine, J. (1957). Study of the soils of the Cheliff plains. PhD Thesis, University of Algiers, Algeria. 582p.
- Bouzelboudjen, M. (1987). Hydrogeology and balance of the El Amra-El Abadia aquifer by mathematical models (Middle Cheliff basin, Algeria), PhD Thesis, University of Franche-Comté, France. 197p.
- Busico, G., Kazakis, N., Cuoco, E., Colombani, N., Tedesco, D., Voudouris, K., & Mastrocico, M. (2020). A novel hybrid method of specific vulnerability to anthropogenic pollution using multivariate statistical and regression analyses. *Water Research*, 171, 115386. <https://doi.org/10.1016/j.watres.2019.115386>
- Busico, G., Mastrocico, M., Cuoco, E., Sirna, M., & Tedesco, D. (2019). Protection from natural and anthropogenic sources: A new rating methodology to delineate "Nitrate vulnerable zones". *Environmental Earth Sciences*, 78(4) doi:10.1007/s12665-019-8118-2
- Djabri, L. (1996). Water pollution of the Seybouse valley - Guelma - Boucheougouf - Annaba regions, its geological, industrial, agricultural and urban origins. PhD Thesis, University of Annaba, Algeria. 247p.
- El Jihad, M.D., & Taabni, M. (2019). L'eau au Maghreb : Quel mix l'hydrique face aux effets du changement climatique ? Eau et climat en Afrique du Nord et au Moyen Orient. "Water in the Maghreb: What "mix" facing the effects of climate change ? Water and climate in North Africa and the Middle East". Editions Transversal: 1-25p.
- Erostate, M., Huneau, F., Garel, E., Vystavna, Y., Santoni, S., & Pasqualini, V. (2019). Coupling isotope hydrology, geochemical tracers and emerging compounds to evaluate mixing processes and groundwater dependence of a highly anthropized coastal hydrosystem. *Journal of Hydrology*, 578, 123979. <https://doi.org/10.1016/j.jhydrol.2019.123979>
- FAO. (2016). <http://www.fao.org/nr/water/aquastat/data/query/index.html?lang=fr>
- Ghebouli, M.S., & Bencheikh Elhocine, M. (2008). Origin of groundwater salinity. The case of Setif high plains (Eastern Algeria). *Sciences & Technologie*, 8, 37–46.
- Gouaïdia, L. (2008). Influence of the lithology and climatic conditions on the variation of the physico-chemical parameters of the aquifers in semi-arid zone, case of the Meskiana aquifer (North-East Algeria). PhD Thesis, University of Annaba, Algeria. 199p.
- IFES. (2002). Design Office, Miliana. Report of geophysical study by electrical prospection of the middle Cheliff (El Attaf), Algeria.
- Jawadi, I., & Gaaloul, N. (2020). Qualitative and quantitative study of water resources in the Sidi Bouzid plain (central Tunisia). *Journal International Sciences et Technique de l'Eau et de l'Environnement*, 15(2), 109–114.
- Johnbosco, C., Egbueri, J.C., Agbasi, D.A., Ayejoto, M.I.K., & Khan, M.Y.A. (2023). Extent of anthropogenic influence on groundwater quality and human health-related risks: an integrated assessment based on selected physicochemical characteristics. *Geocarto International*, 38, 1. <https://doi.org/10.1080/10106049.2023.2210100>
- Kanellopoulos, C., & Argyraki, A. (2022). Multivariate statistical assessment of groundwater in cases with ultramafic rocks and anthropogenic activities influence. *Applied Geochemistry*, 141, 105292. <https://doi.org/10.1016/j.apgeochem.2022.105292>
- Khan, M.Y.A., ElKashouty, M., & Bob, M. (2020). Impact of rapid urbanization and tourism on the groundwater quality in Al Madinah city, Saudi Arabia: a monitoring and modeling approach. *Arabian Journal of Geosciences*, 13, 922. <https://doi.org/10.1007/s12517-020-05906-6>
- Khan, M.Y.A., El Kashouty, M., Gusti, W., Kumar, A., Subyani, A.M., & Alshehri, A. (2022). Geo-Temporal Signatures of Physicochemical and Heavy Metals Pollution in Groundwater of Khulais Region - Makkah Province, Saudi Arabia. *Frontiers in Environmental Science*, 9, 800517. <https://doi.org/10.3389/fenvs.2021.800517>
- Khan, M.Y.A., ElKashouty, M., Subyani, A.M., & Tian F. (2023). Spatio-temporal evaluation of trace element contamination using multivariate statistical techniques and health risk assessment in groundwater, Khulais, Saudi Arabia. *Applied Water Science*, 13, 123. <https://doi.org/10.1007/s13201-023-01928-z>
- Kireche, O. (1977). Geological and structural study of the massifs with schistosity of Cheliff. PhD Thesis, University of USTHB/Algiers, Algeria. 199p.
- Lentini, A., Meddi, E., Galve, J.P., Papiccio, C., & La Vigna, F. (2022). Preliminary identification of areas suitable for Sustainable Drainage Systems and Managed Aquifer Recharge to mitigate storm water flooding phenomena in Rome (Italy). *Acque Sotterranee - Italian Journal of Groundwater*, 11(4), 43–53. <https://doi.org/10.7343/as-2022-590>
- Madene, E., Meddi, H., Boufekane, A., & Meddi, M. (2020). Contribution of hydrogeochemical and isotopic tools to the management of Upper and Middle Cheliff Aquifers. *Journal of Earth Science*, 31(5), 993–1006. <https://doi.org/10.1007/s12583-020-1293-y>
- Madene, E., Boufekane, A., Meddi, M., Busico, G., & Zghib, A. (2022). Spatial analysis and mapping of the groundwater quality index for drinking and irrigation purpose in the alluvial aquifers of upper and middle Cheliff basin (north-west Algeria). *Water Supply*, 22(4), 4422–4444. <https://doi.org/10.2166/ws.2022.107>
- Mastrocico, M., Gervasio, M.P., Busico, G., & Colombani, N. (2021). Natural and Mastrocico, M., Gervasio, M. P., Busico, G., & Colombani, N. (2021). Natural and the Campania plains (southern Italy). *Science of the Total Environment*, 758, 144033. <https://doi.org/10.1016/j.scitotenv.2020.144033>
- Mattauer, M. (1958). Geological study of the eastern Ouarsenis (Algeria). Pub. Serv. Map Algeria. PhD Thesis. University of Paris, France. 343p.
- Meghraoui, M. (1982). Neotectonic study of the northwestern region of El Asnam. Relation with the earthquake of October 10, 1980. PhD Thesis, University of Paris VII, France. 182p.
- Mehdaoui, R., Mili, E.M., & Mahboub, A. (2019). Using physico-chemical and bacteriological parameters to characterize the quality of groundwater in the Ziz Valley (Errachidia province South-East of Morocco). *La Houille Blanche*, 5-6, 5–15. <https://doi.org/10.1051/lhb/2019054>
- Messelmi, H. (2012). Evolution physico-chimique des eaux souterraines des différentes aquifères du Moyen Cheliff. "Physico-chemical evolution of groundwater in the different aquifers of Middle Cheliff". Mémoire de Master, Université Khemis Miliana, Algérie. 154p.

- National Water Resources Agency (NWRA). (2015). Internal document: Climatic data 1971–2017. Geological and geophysical sections. Hydrogeological Yearbook of the upper and middle Cheliff alluvial aquifer. 14–17.
- Orecchia, C., Giambastiani, B.M.S., Greggio, N., Campo, B., & Dinelli, E. (2022). Geochemical Characterization of Groundwater in the Confined and Unconfined Aquifers of the Northern Italy. *Applied Sciences*, 12, 7944. <https://doi.org/10.3390/app12157944>
- Perrodon, A. (1957). Geological study of the sublittoral Neogene basins of northwestern Algeria. PhD Thesis. University of Paris, France.
- Prabakaran, K., Sivakumar, K., & Aruna, C. (2020). Use of GIS-AHP tools for potable groundwater potential zone investigations - a case study in Vairavanpatti rural area, Tamil Nadu, India. *Arabian Journal of Geosciences*, 13(17), 866. <https://doi.org/10.1007/s12517-020-05794-w>
- Remaoun, M. (2007). Floods and droughts in Algeria, case of the Middle Cheliff. PhD Thesis, University of USTHB/Algiers, Algeria. 231p.
- Rezig, A., Saggai, S., Baloul, D., Dahmani, S., Bouamria, M., & Djafer Khodja, H. (2021). Groundwater pollution risk in the region of Bouira (North-Center of Algeria). *Journal of Fundamental and Applied Sciences*, 13(1), 58–74. <https://doi.org/10.4314/jfas.v13i1.4>
- Richa, A. (2010). Approche de l'origine de la salinité des eaux de la nappe alluviale d'Al Attaf. Mémoire de Magister. "Approach to the origin of salinity in the water of the alluvial aquifer of Al Attaf." Université Khemis Miliana, Algérie. 163p.
- Rodier, J. (1996). Water analysis, natural water, waste water, sea water. Edition Dunod, Paris, France. 1383p.
- Rodier, J., Legube, B., Merlet, M., & Brunet, R., (2009). Water analysis. Edition Dunod, Paris, France. 1600p.
- Stafford, J., & Bodson, P. (2006). Multi-varied analysis SPSS. Presses the University of Quebec, Canada. 241p.
- Taherian, P., & Joodavi, A. (2021). Hydrogeochemical characteristics and source identification of salinity in groundwater resources in an arid plain, northeast of Iran: implication for drinking and irrigation purposes. *Acque Sotterranee - Italian Journal of Groundwater*, 10(2), 21–31. <https://doi.org/10.7343/as-2021-502>
- Touhari, F., Meddi, M., Mehaiguene, M., & Razack M. (2015). Hydrogeochemical assessment of the Upper Cheliff groundwater (North West Algeria). *Environmental Earth Sciences*, 73, 3043–3061. <https://doi.org/10.1007/s12665-014-3598-6>
- Vespasiano, G., Muto, F., & Apollaro, C. (2021). Geochemical, Geological and Groundwater Quality Characterization of a Complex Geological Framework: The Case Study of the Coreca Area (Calabria, South Italy). *Geosciences*, 11, 121. <https://doi.org/10.3390/geosciences11030121>
- WHO (2009). Boron in Drinking-water Background document for development of WHO Guidelines for Drinking-water quality Quality. 20p. WHO/HSE/WSH/09.01/2.